JOURNAL OF AIRCRAFT
Vol. 32, No. 5, September–October 1995

Compressibility Effects on Vortex Breakdown Onset Above a 75-Degree Sweep Delta Wing

Miguel R. Visbal* and Raymond E. Gordnier*
U.S. Air Force Wright Laboratory, Wright–Patterson Air Force Base, Ohio 45433-7913

The effects of compressibility on the onset of vortex breakdown above a 75-deg sweep delta wing were explored numerically for both static and pitching conditions. The flows were simulated by solving the mass-averaged, three-dimensional, unsteady Navier–Stokes equations using an implicit, time-accurate Beam–Warming algorithm and the algebraic Baldwin–Lomax turbulence model. Static computations were performed over the freestream Mach number range $0.2 \leq M_\infty \leq 0.95$ and for a chord Reynolds number $Re_C = 2 \times 10^6$. Compressibility was found to have a pronounced effect on the flow structure for static conditions. The formation of several shocks and an embedded supersonic region in the vortex core (for M_∞ as low as 0.4) were encountered prior to the onset of vortex breakdown. Despite these drastic changes in the flow structure, the quasistatic breakdown onset angle varied only slightly. Compressibility effects on the transient onset of vortex breakdown were also investigated for a ramp-type pitch maneuver to high angle of attack with $0.2 \leq M_\infty \leq 0.6$. Under dynamic conditions increasing M_∞ resulted in a larger delay of breakdown and in the formation of a complex, three-dimensional shock structure at $M_\infty = 0.6$. Compressibility effects were found to be similar when comparing the results from laminar and turbulent pitching calculations, indicating that these effects are to a great extent inviscid in nature.

Nomenclature

C	=	wing chord
C_p	=	pressure coefficient, $2(p - p_\infty)/\rho_\infty U_\infty^2$
M	=	Mach number
M_c	=	crossflow Mach number
t	=	time
t^+	=	nondimensional time, tU_∞/C
U, V, W	=	velocity components in wing frame of reference
U_∞	=	freestream velocity
X_b	=	chordwise location of vortex breakdown
X, Y, Z	=	coordinate system attached to the wing
α	=	geometric angle of attack
ξ, η, ζ	=	transformed coordinates
Ω	=	pitch rate, rad/s
Ω^+	=	nondimensional pitch rate, $\Omega C/U_\infty$

Introduction

THE vortical flows encountered by aircraft during high-angle-of-attack maneuvering exhibit a variety of aerodynamic phenomena not yet fully understood.[1,2] Among these complex, three-dimensional, and unsteady flow features, "vortex breakdown" or "vortex bursting" remains a challenge, both in its fundamental understanding, as well as in its prediction and control. Breakdown of leading-edge vortices above slender wings is typically characterized by reverse axial flow in the vortex core and by marked flow fluctuations downstream of the breakdown inception point. Vortex bursting severely impacts aircraft stability and control, and may also promote damaging fluid/structure interactions, resulting in a reduction of the operational envelope and service life of modern fighter aircraft. The need for further experimental and computational study of this phenomenon is apparent.

Presented as Paper 94-0538 at the AIAA 32nd Aerospace Sciences Meeting and Exhibit, Reno, NV, Jan. 10–13, 1994; received Feb. 4, 1994; revision received June 2, 1995; accepted for publication June 2, 1995.

*Research Aerospace Engineer, CFD Research Branch, Aeromechanics Division. Senior Member AIAA.

The majority of experimental studies of vortex breakdown on delta wings have been performed for incompressible flow (i.e., in water facilities) or for low freestream Mach numbers ($M_\infty < 0.2$). Consequently, compressibility effects on the onset and unsteady structure of vortex breakdown for either stationary or maneuvering wings have not been investigated sufficiently. Recently, experimental[3–5] and computational[6,7] studies of transonic flows past a 65-deg sweep delta wing have been conducted. These investigations have shown that compressibility results in significant changes in the flowfield structure for static conditions at angles of attack prior to breakdown onset. A summary of the various flow features as a function of (M_∞, α) has been provided in Ref. 4. Compressibility effects are expected to depend strongly on wing geometry, however, different wing sweeps have not yet been considered. In addition, compressibility effects for maneuvering cases have not been investigated.

The main objective of the present study is to explore the effects of compressibility on the onset of vortex breakdown above a slender delta wing for both static and dynamic (pitching) conditions. Calculations are performed for a 75-deg sweep flat-plate delta wing over the freestream Mach number range $0.2 \leq M_\infty \leq 0.95$ and for a chord Reynolds number $Re_C = 2 \times 10^6$. The flows are simulated by solving the unsteady, three-dimensional, mass-averaged, compressible Navier–Stokes equations using a time-accurate, implicit solver.

Methodology

Governing Equations and Numerical Procedure

The governing equations are the unsteady, three-dimensional, compressible Navier–Stokes equations written in strong conservation law form.[8] Closure of this system of equations is provided by the perfect gas law, Sutherland's viscosity formula, and the assumption of a constant Prandtl number ($Pr = 0.72$). In order to deal with the case of external flow past a body in general motion, a time-dependent coordinate transformation is incorporated. High Reynolds number turbulent flows are simulated using mass-averaged variables and the algebraic eddy viscosity model of Baldwin and Lomax.[9]

The governing equations are numerically solved employing the implicit, approximate-factorization, Beam–Warming al-

gorithm.[10] The scheme is formulated using Euler implicit time differencing and second-order finite difference approximations for all spatial derivatives. A blend of second- and fourth-order nonlinear dissipation is added to control the spurious numerical oscillations.[11] Newton subiterations[12,13] are also incorporated in order to reduce linearization and factorization errors, thereby improving the temporal accuracy and stability properties of the algorithm. The fully vectorized, time-accurate, three-dimensional Navier–Stokes solver has been validated for both steady and unsteady flowfields.[14–16] In particular, Refs. 17–19 describe the application of the algorithm to the case of vortex breakdown at low Reynolds numbers.

Grid Structure and Boundary Conditions

The computational grid topology for the flat-plate delta wing is of the H-H type[13] and is obtained using simple algebraic techniques. Two different grids of sizes 98 × 115 × 102 (grid 1) and 162 × 107 × 151 (grid 2) in the ξ, η, and ζ directions, respectively, are employed to assess resolution effects. The ξ, η, and ζ directions correspond to the streamwise, spanwise, and normal directions relative to the delta wing. For grid 1, the minimum spacing normal to the wing is $\Delta Z/C = 0.0001$, the streamwise spacing on the wing is $\Delta X/C = 0.02$, and the minimum and maximum spanwise spacing on the wing ($\Delta Y/C$) at $X/C = 1.0$ are 0.001 and 0.019, respectively. The far-field boundaries are located one and a half chord lengths away from the delta wing. For grid 2, the minimum spacing normal to the wing is $\Delta Z/C = 5.0 \times 10^{-5}$, the streamwise spacing on the wing is $\Delta X/C = 0.01$, and the minimum and maximum spanwise spacing on the wing ($\Delta Y/C$) at $X/C = 1.0$ are 0.001 and 0.0075, respectively. The upper and downstream portions of the far-field boundary of grid 2 are placed at a distance of four chord lengths away from the wing.

The boundary conditions are implemented in the following manner. On the lower, upper, lateral, and upstream boundaries, characteristic conditions are specified. On the downstream boundary, through which the vortex exits, flow variables are extrapolated from the interior. Symmetry conditions are imposed along the midplane of the wing. On the wing surface, the following conditions are applied:

$$u = u_b$$

$$T = T_a$$

$$\frac{\partial p}{\partial \zeta} = -\rho \boldsymbol{a}_b \cdot \hat{n}$$

where $\hat{n}$ denotes the surface normal, T_a is the adiabatic wall temperature, and $\boldsymbol{u}_b$ and $\boldsymbol{a}_b$ are the velocity and acceleration at the surface of the pitching wing given by

$$\boldsymbol{u}_b = \boldsymbol{\Omega} \times (\boldsymbol{r}_b - \boldsymbol{r}_0)$$

$$\boldsymbol{a}_b = \frac{d\boldsymbol{\Omega}}{dt} \times (\boldsymbol{r}_b - \boldsymbol{r}_0) + \boldsymbol{\Omega} \times [\boldsymbol{\Omega} \times (\boldsymbol{r}_b - \boldsymbol{r}_0)]$$

in terms of the instantaneous pitch rate $\boldsymbol{\Omega} = \Omega \hat{j}$ and the pitch axis location $\boldsymbol{r}_0$. For the static cases, $\Omega = 0.0$, whereas for the pitching cases, the specific functional variation of $\Omega(t)$ can be found in Ref. 19.

Results

All calculations were performed for a 75-deg sweep flat-plate delta wing and for a chord Reynolds number $Re_C = 2.0 \times 10^6$. Before addressing compressibility effects on the onset of vortex breakdown, the solution procedure was validated by a numerical resolution study and by comparison with available experimental data.

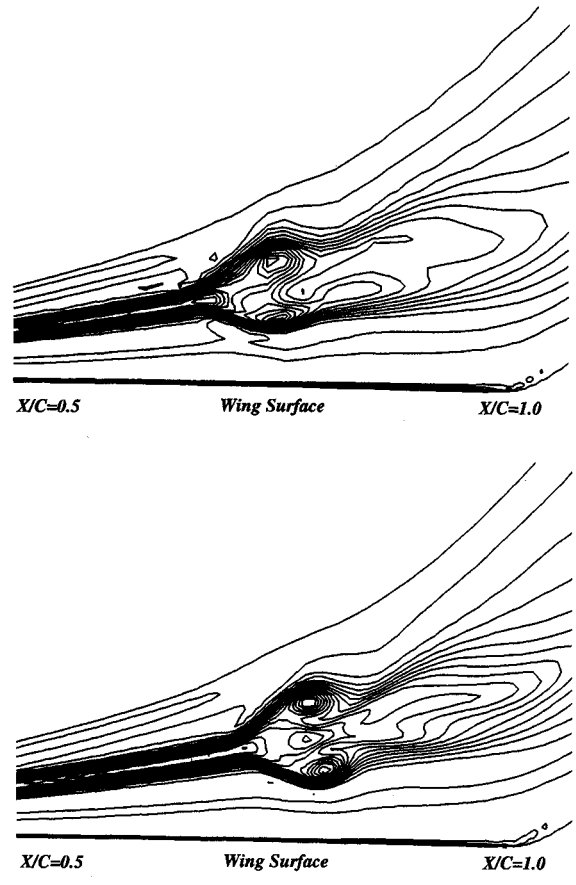

Fig. 1 Effect of grid resolution on vortex breakdown unsteady structure ($M_\infty = 0.2$, $\Omega^+ = 0.3$, $\alpha = 44$ deg): a) grid 1 and b) grid 2.

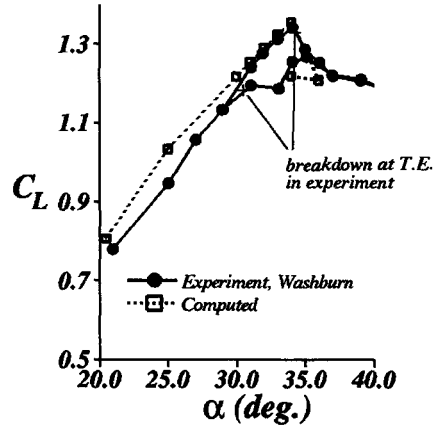

Fig. 2 Comparison of computed and experimental[21] static lift coefficients.

The effect of grid resolution on the computed static solutions at $\alpha = 25$ deg was investigated for $M_\infty = 0.2$ and 0.6. The surface pressure distributions computed using both grids were examined and found[20] to display little sensitivity to grid refinement, with the exception of the maximum suction peak. At the chordwise station $X/C = 0.5$, for instance, the maximum variation with grid refinement in the magnitude of the surface pressure coefficient was found to be of the order of 5%.

The influence of grid spacing on the computed instantaneous vortex breakdown structure was also investigated for the pitching cases. An example of grid resolution effects is given in Fig. 1, which shows total pressure contours on a longitudinal plane through the vortex core for $M_\infty = 0.2$ and $\Omega^+ = 0.3$ at $\alpha = 44$ deg. On the coarser grid, the breakdown

Table 1 Summary of computed static cases

α, deg	M_∞ 0.2	0.4	0.6	0.8	0.9	0.95
25	——	——	b	b, c, d	b, c, d, g	b, c, d, g, h
30	——	NC	NC	b, c, d	NC	b, c, d, e, f, g, h
31	——	NC	NC	NC	NC	NC
32	——	NC	NC	NC	NC	b, c, d, e, f, g, h
33	——	NC	NC	NC	NC	a
34	——	b	b, c, d	b, c, d, e, f	NC	NC
35	a	b	b, c, d	a	NC	NC
36	NC	a	a	NC	NC	NC

a, Quasistatic onset of breakdown; b, $M > 1$ in core; c, $M > 1$ in symmetry plane; d, lower crossflow shock; e, centerline shock; f, upper crossflow shock; g, trailing-edge shock; h, terminal shock; NC, not computed.

region is located slightly upstream of the finer grid solution. However, the overall flow structure on both grids is found to be in reasonable agreement.

Comparison of the computed lift coefficient for the static cases corresponding to $M_\infty = 0.2$ with the experimental data of Washburn[21] is presented in Fig. 2. The computed lift coefficient and lift stall onset are found to be in fairly good agreement with the experiment. The movement of vortex breakdown past the trailing edge is reported in the experiment to take place at $\alpha = 34.5$ deg, as the angle of attack is increased slowly. In the computations, the onset of vortex breakdown occurs when α is increased from 34 to 35 deg, in close agreement with the experiment. Despite the reasonable agreement with the experiment, given the uncertainties associated with turbulence modeling, the following description of the computed flowfields will be limited to the onset and early stages of vortex breakdown.

Static Cases

In order to investigate the effects of compressibility on the onset of vortex breakdown for static conditions, computations were performed over the freestream Mach number range $0.2 \leq M_\infty \leq 0.95$. A summary of all cases computed is provided in Table 1. Given the large number of calculations required, the numerical results were obtained on the coarser grid (grid 1) previously described. In addition, in the vicinity of breakdown onset, the angle of attack was varied in 1-deg increments, and therefore, the results may be considered to be quasistatic. Although smaller α increments would be desirable, this was found to be computationally prohibitive.

The effect of compressibility on the flow structure prior to the static onset of breakdown was examined by comparing the solutions obtained at $\alpha = 25$ deg. The surface pressure coefficient at $X/C = 0.5$ is shown for all M_∞ in Fig. 3a. As M_∞ is increased the minimum pressure peak decreases and moves slightly inboard. The line of secondary separation on the wing upper surface (not shown) was also found to move inboard with increasing M_∞, and for $M_\infty > 0.8$, it was located at the foot of the crossflow shock that appeared underneath the leading-edge vortex (as described later). The pressure along a streamline released in the center of the vortex core was also examined. The streamline trajectories displayed an inboard displacement with increasing M_∞ consistent with that found for the surface pressure (Fig. 3a). The pressure distributions along the vortex core (Fig. 3b) became progressively flatter with increasing Mach number, indicating a diminishing upstream influence of the wing trailing edge and a corresponding reduced adverse pressure gradient in the axial direction. This behavior is associated with the formation, within the primary vortex core, of an embedded supersonic region that extends from very close to the apex, past the wing trailing edge, and into the near wake. The maximum Mach number in the leading-edge vortex core, as a function of M_∞, is shown in Fig. 4. For $\alpha = 25$ deg, the flow is already supersonic in the vortex core for $M_\infty = 0.6$.

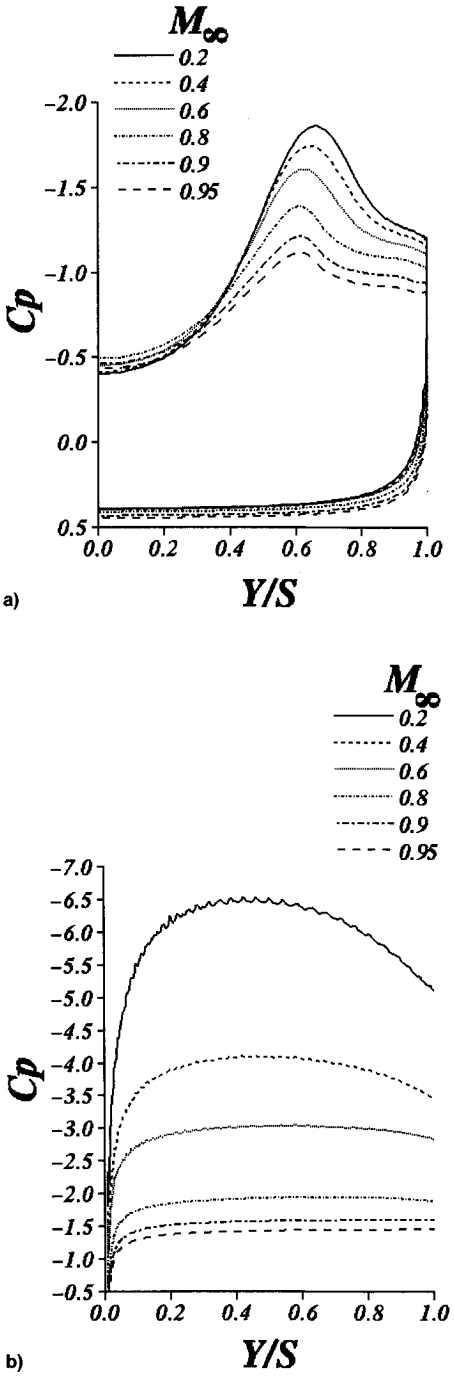

Fig. 3 Effect of freestream Mach number for $\alpha = 25$ deg: a) surface pressure distribution at $X/C = 0.5$ and b) pressure distribution along vortex core.

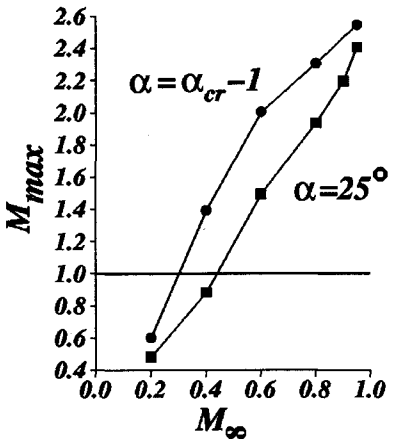

Fig. 4 Variation of maximum Mach number in the vortex core as a function of M_∞.

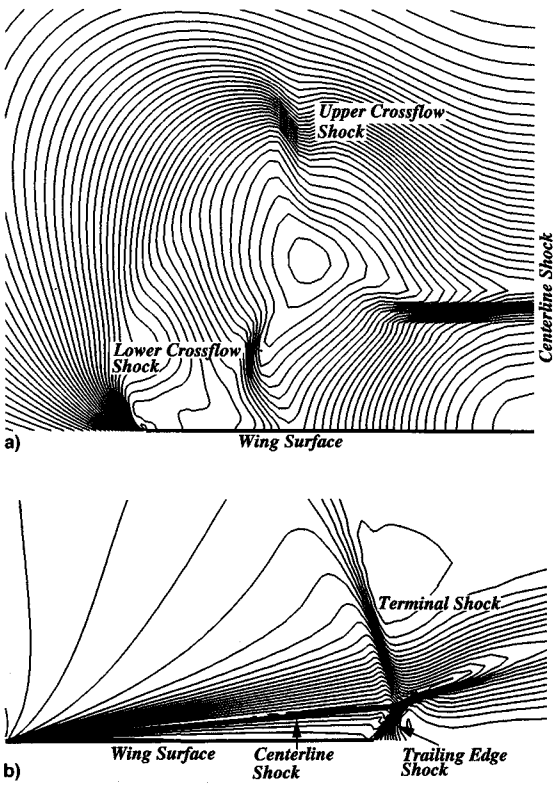

Fig. 5 Computed shock structure for $M_\infty = 0.95$ and $\alpha = 30$ deg. C_p contours on a) crossflow plane $X/C = 0.5$ and b) symmetry plane.

Examination of the computed flowfields prior to the onset of breakdown revealed that with increasing freestream Mach number and incidence several complex shock structures are formed above the wing. A summary of when these shocks appeared as a function of M_∞ and α is provided in Table 1. Only the most complex shock structure, obtained for $M_\infty = 0.95$ and $\alpha = 30$ deg, is shown in Fig. 5. The pressure contour plot on a transverse plane at $X/C = 0.5$ (Fig. 5a) indicates the formation of crossflow shocks between the primary vortex and the wing (denoted as the "lower crossflow shock"), as well as above the vortex (denoted as the "upper crossflow shock"). The lower crossflow shock is the first shock structure that develops with increasing Mach number (see Table 1), and has also been observed experimentally[4,5] for a 65-deg sweep delta wing. Reference 5 also reports the existence of the upper crossflow shock for a LEX-wing configuration. Another prominent shock structure, denoted as the "centerline shock," is quite apparent in Figs. 5a and 5b. This type of shock has been observed in experiments[22] for supersonic flow ($M_\infty = 2.5$) past a 73-deg sweep wing and is discussed in more detail for the pitching case at $M_\infty = 0.6$. For the present wing sweep, the centerline shock is found to be the strongest shock structure.

For the higher values of freestream Mach number considered ($M_\infty = 0.9$ and 0.95), turning of the supersonic flow in the trailing-edge region resulted in the formation of an oblique shock denoted as the "trailing-edge shock." This type of shock can be clearly seen for $M_\infty = 0.95$ in the symmetry-plane pressure contours of Fig. 5b. Finally, for $M_\infty = 0.95$, an additional shock (denoted as the "terminal shock") is observed (Fig. 5b) near the trailing-edge region and above the centerline shock. This shock structure bears resemblance to the typical terminal shock found in transonic airfoil flow.

From the previous description of the computed flowfields it is apparent that compressibility has a significant effect on the flow structure above the wing. The variation (with M_∞) of the maximum Mach number in the vortex core, shown in Fig. 4, indicates that a supersonic core is present prior to the onset of breakdown for freestream Mach numbers above 0.3. In addition, the formation of the shock structures previously noted results in the loss of approximate axial symmetry displayed by the primary vortex core at low Mach numbers.

The effect of compressibility on the quasistatic onset of breakdown is summarized in Table 1. The maximum variation in onset angle (α_{cr}) over the freestream Mach number range considered was only 3 deg. Increasing M_∞ (up to 0.6) results initially in a very small breakdown delay, followed by a drop in α_{cr} for $M_\infty = 0.8$ and 0.95. The computed small effect of freestream Mach number on α_{cr}, as well as the trend, are similar to those found in the experiments[4] for a $\Lambda = 65$-deg sweep wing.

The effect of hysteresis on the onset of breakdown was also considered. As shown in Fig. 2, in the experiment of Washburn,[21] breakdown crosses the trailing edge when increasing α at $\alpha_{cr} = 34.5$ deg. However, breakdown does not move into the wake until the angle of attack is reduced to 31 deg. In the present computations for $M_\infty = 0.2$, breakdown occurs in the near-wake and moves onto the wing when the angle of attack is increased from 34 to 35 deg. However, when incidence is decreased from 36 to 34 deg, a mean flow solution containing breakdown is attained. The corresponding computed lift hysteresis is shown in Fig. 2. Hysteresis in lift and in the onset of vortex breakdown was also obtained computationally for $M_\infty = 0.6$. Further computational and experimental work are, however, required to confirm this behavior.

Pitching Cases

The effect of compressibility on the onset of vortex breakdown was also investigated under pitching conditions. Computations were performed at three different freestream Mach numbers ($M_\infty = 0.2$, 0.4, and 0.6) for a ramp-type, pitch-and-hold maneuver from $\alpha = 25$ to 50 deg. The wing pitch rate increased smoothly from zero to a constant value $\Omega^+ = \Omega C/U_\infty = 0.3$, and then decelerated as the final incidence was reached. The specific variation of $\Omega(t)$ is given in Ref. 19. For all cases, the pitch axis was located at the wing apex. The pitching calculations, performed using the two grids previously described, were found in reasonable agreement. Therefore, only the results obtained on the finer grid (grid 2) are included in this section.

The effect of freestream Mach number variation on the onset of vortex breakdown for the pitching cases is shown in Fig. 6. It is clearly seen that increasing M_∞ results in a delay of breakdown. This delay is particularly pronounced for $M_\infty = 0.6$ in which case breakdown does not occur above the wing until the pitching motion has ended at $\alpha = 50$ deg.

The effect of compressibility on the onset of vortex breakdown is illustrated further in Fig. 7, which shows contours of

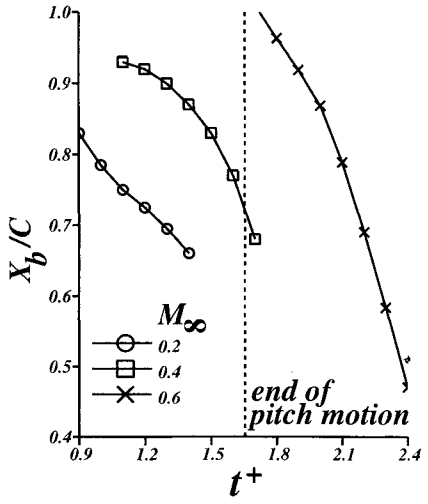

Fig. 6 Effect of compressibility on transient vortex breakdown location for pitching cases.

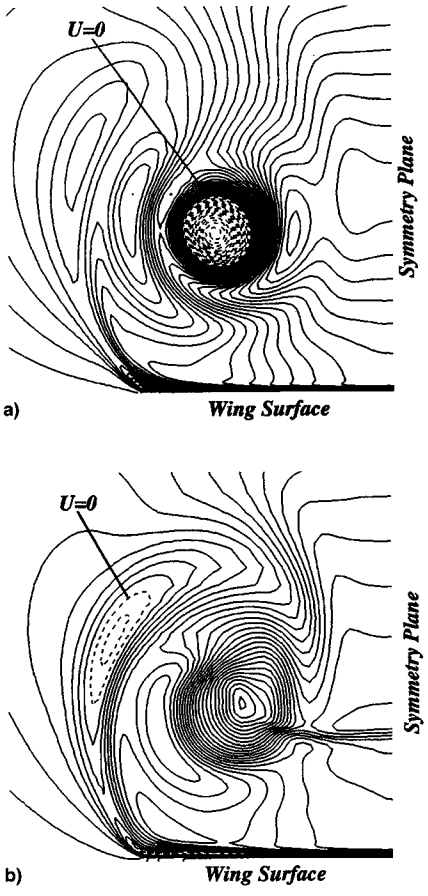

Fig. 7 Effect of compressibility on instantaneous flow structure on crossflow plane $X/C = 0.97$ ($\alpha = 44$ deg, $\Omega^+ = 0.3$). M_∞ = a) 0.2 and b) 0.6.

the U component of velocity on the chordwise plane $X/C = 0.97$ at $\alpha = 44$ deg. For $M_\infty = 0.2$ (Fig. 7a), the onset of reverse flow appears in the center of the vortex core, as normally assumed. However, for $M_\infty = 0.6$ (Fig. 7b), reverse flow is initially present away from the center of the vortex in the shear layer region emanating from the leading edge. This difference in the onset of reversed flow is associated with the presence of the supersonic region in the vortex core and the accompanying less severe adverse pressure gradient along the axis.

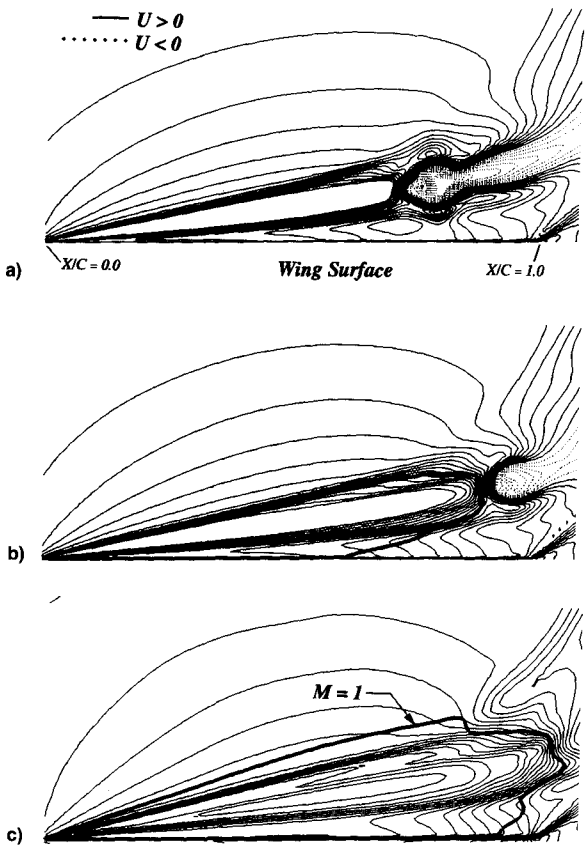

Fig. 8 Effect of compressibility on instantaneous flow structure on longitudinal plane through vortex core ($\alpha = 44$ deg, $\Omega^+ = 0.3$). M_∞ = a) 0.2, b) 0.4, and c) 0.6.

The flow structure for the three different Mach numbers is compared in Fig. 8 at $\alpha = 44$ deg. This figure shows contours of the U component of velocity on a longitudinal plane through the vortex core as well as the $M = 1$ contour (thick line) for $M_\infty = 0.4$ and $M_\infty = 0.6$. The delay of vortex bursting with increasing Mach number is readily apparent. For $M_\infty = 0.2$, the flow is entirely subsonic ($M_{max} = 0.85$), however, for $M_\infty = 0.4$ a large region of supersonic flow already exists in the vortex core with $M_{max} = 1.63$. For $M_\infty = 0.6$, this supersonic region extends past the trailing edge of the wing and $M_{max} = 2.18$. Examination of the flow structure on the $X/C = 0.5$ plane did not reveal the formation of well-defined crossflow shocks for $M_\infty = 0.4$, since the corresponding maximum crossflow Mach number was only slightly supersonic ($M_{c\,max} = 1.08$). However, for $M_\infty = 0.6$, several shocks were found, as described next.

Details of the three-dimensional shock structure for $M_\infty = 0.6$ at $\alpha = 44$ deg are presented in Fig. 9. The most prominent shock structure is the centerline shock clearly seen on the symmetry plane (Fig. 9a). This shock (which is initially oblique), emanates near the apex and extends in an approximate conical fashion over a major portion of the wing before terminating, as a nearly normal shock, just upstream of the trailing edge. The instantaneous streamlines in Fig. 9a show that the centerline shock is associated with the turning of the flow in a direction parallel to the wing surface. Contrary to the interpretation given in Ref. 22, this turning is accomplished both by this shock and by the subsequent compression between the shock and the surface. The centerline shock is also clearly visible in the pressure coefficient plot on a crossflow plane (Fig. 9b) where it appears parallel to the wing surface and extending across the symmetry plane.

An upper crossflow shock as well as a weak lower crossflow shock are also evident in Fig. 9b. The upper crossflow shock is associated with the deceleration of the swirling flow as it

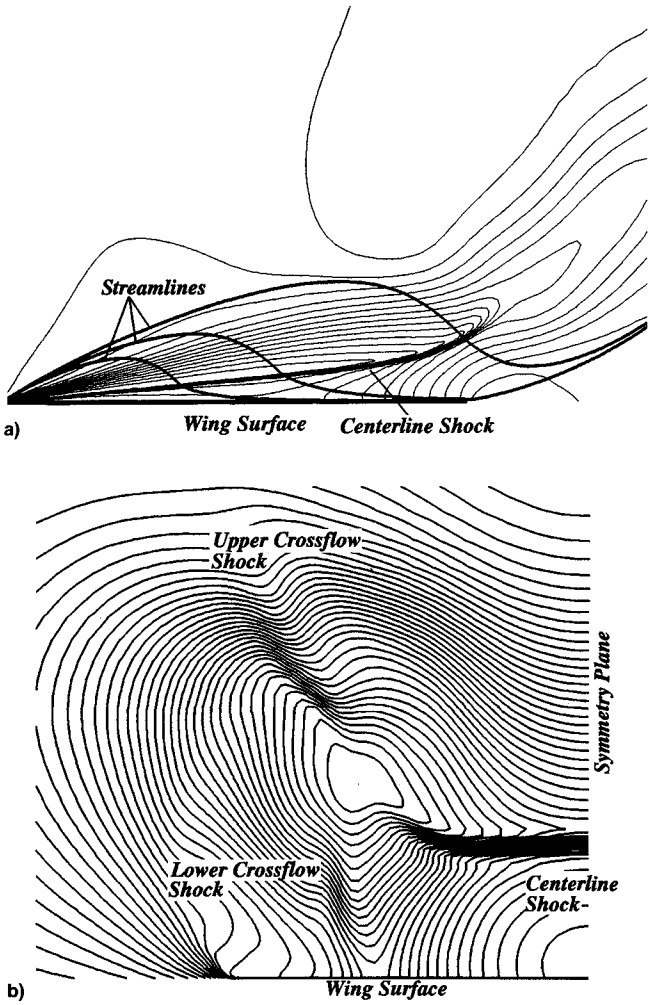

Fig. 9 Shock structure above pitching wing for $M_\infty = 0.6$ and $\alpha = 44$ deg. C_p contours on a) symmetry plane and b) crossflow plane $X/C = 0.85$.

approaches the plane of symmetry, and at the instant under consideration, extended from approximately $X/C = 0.15$ to $X/C = 0.95$.

Based on the flow structure for both $M_\infty = 0.4$ and 0.6 on a longitudinal plane through the vortex core (Figs. 8b and 8c), an additional normal shock of limited radial extent is also expected to terminate the supersonic region in the core, as the axial flow decelerates and encounters breakdown. For the present grid resolution and numerical scheme, it is difficult to separate this terminating shock from the strong compression that takes place just upstream of breakdown. A dynamically adapting grid might be required near the nose of the upstream-moving breakdown in order to clearly delineate this additional feature.

In order to test the dependence of the compressibility effects on Reynolds number, computations were also performed[20] for laminar flow at $Re_C = 9.2 \times 10^3$ and for freestream Mach numbers of 0.2 and 0.6. Comparison of these cases again revealed a delay in the transient onset of vortex breakdown with increasing freestream Mach number. In addition, the three-dimensional shock structure for the laminar case at $M_\infty = 0.6$ was examined and found to be in qualitative agreement with the corresponding high Reynolds number structure, shown in Fig. 9. Therefore, the trends observed in the present study with increasing M_∞ are to a great extent inviscid in nature.

Concluding Remarks

The effects of compressibility on the onset of vortex breakdown above a 75-deg sweep delta wing were investigated numerically for both static and dynamic (pitching) conditions. For static cases, computations were performed over the freestream Mach number range $0.2 \leq M_\infty \leq 0.95$, and for angles of attack up to the onset of breakdown. Compressibility had a dramatic effect on the flow structure above the wing and several types of shocks appeared with increasing M_∞ and angle of attack. An embedded supersonic region formed within the leading-edge vortex prior to the onset of breakdown for freestream Mach numbers as low as 0.4. Despite the pronounced effect of compressibility on the flow structure, the quasistatic breakdown onset angle displayed only a modest 3-deg variation over the Mach number range considered. Hysteresis in lift and breakdown onset were also computed for $M_\infty = 0.2$ and 0.6.

Compressibility effects were explored for a high-rate, ramp-type, pitch maneuver to high angle of attack over the freestream Mach number range $0.2 \leq M_\infty \leq 0.6$. Increasing M_∞ resulted in a delay of the dynamic onset of vortex breakdown over the pitching wing. The same qualitative three-dimensional shock structure was found in both laminar and turbulent pitching calculations, indicating little sensitivity to viscous effects. Experimental work is clearly required to confirm these compressibility effects and to provide validation of the computational approach.

Acknowledgments

This work was supported in part by a Grant of HPC time from the DoD HPC Shared Resource Centers CEWES at Vicksburg, Mississippi and NAVOCEANO at Bay St. Louis, Mississippi. The authors are grateful to Datta Gaitonde for several helpful conversations.

References

[1]Skow, A. M., and Erickson, G. E., "Modern Fighter Aircraft Design for High-Angle-of-Attack Maneuvering," AGARD LS-121, Paper 4, 1982.

[2]Rockwell, D., "Three-Dimensional Flow Structure on Delta Wings at High Angle of Attack: Experimental Concepts and Issues," AIAA Paper 93-0550, Jan. 1993.

[3]Bannink, W. J., Houtman, E. M., and Ottochian, S. P., "Investigation of the Vortex Flow over a Sharp-Edged Delta Wing in the Transonic Regime," Faculty of Aerospace Engineering, Delft Univ. of Technology, Rept. LR-594, Delft, The Netherlands, Oct. 1989.

[4]Elsenaar, A., and Hoeijmakers, H., "An Experimental Study of the Flow over a Sharp-Edged Delta Wing at Subsonic and Transonic Speeds," AGARD CP-494, 1990.

[5]Erickson, G., Schreiner, J., and Rogers, L., "On the Structure, Interaction, and Breakdown Characteristics of Slender Wing Vortices at Subsonic, Transonic, and Supersonic Speeds," AIAA Paper 89-3345, Aug. 1989.

[6]Van den Berg, J. I., Hoeijmakers, H. W. M., and Brandsma, F. J., "Numerical Investigation into Vortical Flow About a Delta-Wing Configuration up to Incidences at Which Vortex Breakdown Occurs in Experiment," AIAA Paper 94-0621, Jan. 1994.

[7]Kandil, O. A., Kandil, H. A., and Liu, C. H., "Shock-Vortex Interaction over a 65-Degree Delta Wing in Transonic Flow," AIAA Paper 93-2973, July 1993.

[8]Pulliam, T. H., and Steger, J. L., "Implicit Finite-Difference Simulation of Three-Dimensional Compressible Flow," *AIAA Journal*, Vol. 18, No. 2, 1980, pp. 159–167.

[9]Baldwin, B., and Lomax, H., "Thin Layer Approximation and Algebraic Model for Separated Turbulent Flows," AIAA Paper 78-257, Jan. 1978.

[10]Beam, R. M., and Warming, R. F., "An Implicit Factored Scheme for the Compressible Navier-Stokes Equations," *AIAA Journal*, Vol. 16, No. 4, 1978, pp. 393–402.

[11]Pulliam, T., "Artificial Dissipation Models for the Euler Equations," *AIAA Journal*, Vol. 24, No. 12, 1986, pp. 1931–1940.

[12]Rai, M., and Chakravarthy, S., "An Implicit Form of the Osher Upwind Scheme," *AIAA Journal*, Vol. 24, No. 5, 1986, pp. 735–743.

[13]Gordnier, R. E., and Visbal, M. R., "Unsteady Vortex Structure over a Delta Wing," *Journal of Aircraft*, Vol. 31, No. 1, 1994, pp.

243–248; also AIAA Paper 91-1811, June 1991.
[14]Webster, W. P., and Shang, J. S., "Comparison Between Thin-Layer and Full Navier-Stokes Simulations over a Supersonic Delta Wing," *AIAA Journal*, Vol. 29, No. 9, 1991, pp. 1363–1369.
[15]Visbal, M., "Structure of Laminar Juncture Flows," *AIAA Journal*, Vol. 29, No. 8, 1991, pp. 1273–1282.
[16]Stanek, M., and Visbal, M., "Investigation of Vortex Development on a Pitching Slender Body of Revolution," *Journal of Aircraft*, Vol. 30, No. 5, 1993, pp. 711–718.
[17]Visbal, M. R., "Onset of Vortex Breakdown Above a Pitching Delta Wing," *AIAA Journal*, Vol. 32, No. 8, 1994, pp. 1568–1575.
[18]Visbal, M. R., "Computational Study of Vortex Breakdown on a Pitching Delta Wing," AIAA Paper 93-2974, July 1993.
[19]Visbal, M. R., and Gordnier, R. E., "Pitch Rate and Pitch-Axis Location Effects on Vortex Breakdown Onset," *Journal of Aircraft*, Vol. 32, No. 5, 1995, pp. 929–935.
[20]Visbal, M. R., and Gordnier, R. E., "Parametric Effects on Vortex Breakdown over a Pitching Delta Wing," AIAA Paper 94-0538, Jan. 1994.
[21]Washburn, A. E., "Effects of External Influences on Subsonic Delta Wing Vortices," AIAA Paper 92-4033, July 1992.
[22]Szodruch, J., and Ganzer, U., "On the Lee-Side Flow over Delta Wings at High Angle of Attack," *High Angle of Attack Aerodynamics*, CP-247, AGARD, 1979 (Paper 21).